Lanthanides

DOI: 10.1002/anie.200902045

A Miniaturized Linear pH Sensor Based on a Highly Photoluminescent Self-Assembled Europium(III) Metal–Organic Framework**

Bogdan V. Harbuzaru, Avelino Corma, Fernando Rey, Jose L. Jordá, Duarte Ananias, Luis D. Carlos, and João Rocha**

The field of lanthanide-based metal–organic frameworks (LnMOFs) with two- or three-dimensional structures[1–4] is rapidly growing because of the discovery of new crystalline structures that exhibit interesting properties and have potential applications in catalysis,[5–13] sensors,[14–19] contrast agents,[20] non-linear optics,[21,22] displays,[23] and electroluminescent devices.[24] For photoluminescence applications, it is necessary to prepare lanthanide-containing materials with high quantum efficiencies, in order to achieve the required miniaturization and reduce energy losses from undesirable quenching processes.[25] Moreover, it is highly desirable to combine the properties of ligands and antennae in one organic moiety. A well-known powerful sensitizing ligand for Eu^{3+} ions in solution is 1,10-phenanthroline-2,9-dicarboxylic acid (H_2PhenDCA), in which both carboxylic and phenanthroline moieties may coordinate to the metal center.[26,27] The proximity between the coordinative parts means that this chelating agent has the tendency to form zero-dimensional (molecular) complexes that are useful in some solution-based analytical applications, but cannot be applied as solid sensors or light-emitting materials. Thus, it is of interest to obtain the two- or three-dimensional insoluble counterparts of these zero-dimensional water-soluble complexes. To achieve this goal, we have used hydrothermal synthesis, which is a powerful technique for the preparation of metastable compounds that may not be accessible by using conventional methods.[28,29] Hydrothermal synthesis also allows the use of chelating agents that are sparingly soluble in water at temperatures below 373 K, thus enhancing the lanthanide-coordinating ability of the ligand.

Herein, we report the synthesis, structure, and sensing properties of a new Eu^{3+} metal–organic framework ITQMOF-3-Eu (ITQMOF = Instituto de Tecnologia Quimica Metal Organic Framework) that contains the ligand 1,10-phenanthroline-2,9-dicarboxylic acid. The excellent balance between absorption, energy transfer, and emission rate of the Eu^{3+} ITQMOF-3 (ITQMOF-3-Eu) allowed the fabrication of a miniaturized pH sensor prototype that functions in the biologically interesting range (5–7.5). By combining this material and an optical fiber, a linear photoluminescence response, which also allows the self-calibration of the emitting signal within this pH range, was achieved. The ITQMOF-3-Eu material was obtained by reacting the H_2PhenDCA ligand and the Eu^{3+} salt or oxide under hydrothermal conditions (see the Supporting Information). The crystal has a strong red luminescence under ultraviolet light (see Figure 1 a). Chemical and elemental analyses showed that the formula of the material is $[Eu_3(C_{14}H_6N_2O_4)_4(OH)(H_2O)_4]\cdot 2\,H_2O$.

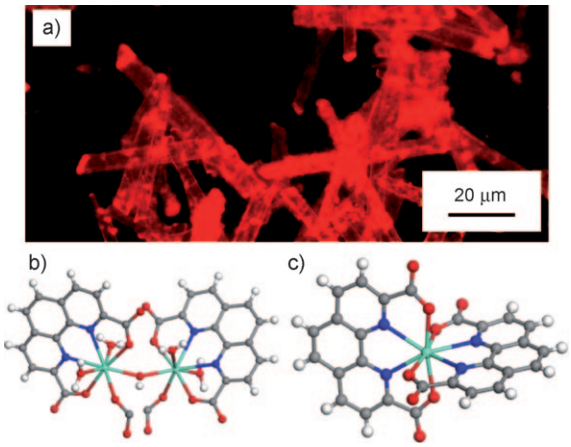

Figure 1. a) Optical microscopy image of ITQMOF-3-Eu under UV light. b) Eu2 coordination environment. c) Eu1 coordination environment. C gray, H white–gray, N blue, Eu green, O red.

The structure of ITQMOF-3-Eu was determined from single-crystal X-Ray diffraction data[30] (collected at Beamline BM16 at ESRF) using SHELXS-97[31] and refined with SHELXL-97.[32] The structure was indexed using an orthorhombic unit cell with $a = 15.625$ Å, $b = 31.237$ Å, $c = 10.847$ Å; the space group $Ccc2$ (no. 37) was assigned according to the systematic extinctions in the diffraction patterns.

ITQMOF-3 can be described as a layered compound with two well-defined and very different sheets, A and B. Each sheet contains one type of Eu^{3+} ion (either Eu1 or Eu2) in a

[*] Dr. B. V. Harbuzaru, Prof. Dr. A. Corma, Dr. F. Rey, Dr. J. L. Jordá
Instituto de Tecnología Química, (UPV-CSIC)
Universidad Politécnica de Valencia
Avda. de los Naranjos s/n, 46022 Valencia (Spain)
Fax: (+34) 96-387-7809
E-mail: acorma@itq.upv.es
Dr. D. Ananias, Prof. Dr. L. D. Carlos, Prof. Dr. J. Rocha
Departments of Chemistry and Physics, CICECO
University of Aveiro, 3810-193 Aveiro (Portugal)

[**] We thank the European Network of Excellence FAME and Beamline BM-16 at ESRF in Grenoble for beam time allocation. B.V.H., A.C., J.L.J., and F.R. would like to thank PROMETEO, Fundacion Areces, and Spanish CICYT (MAT2006-08039, M0ZAT2006-14274-C02-01) for financial support. D.A., L.D.C., and J.R. thank FCT and PTDC. We also thank F. J. Martinez-Casado for helpful discussions.

Supporting information for this article is available on the WWW under http://dx.doi.org/10.1002/anie.200902045.

different crystallographic position (Figures 1 and 2). Sheet A, which contains Eu1, has an ML_2 stoichiometry (M = lanthanide and L = ligand PhenDCA) and is negatively charged.

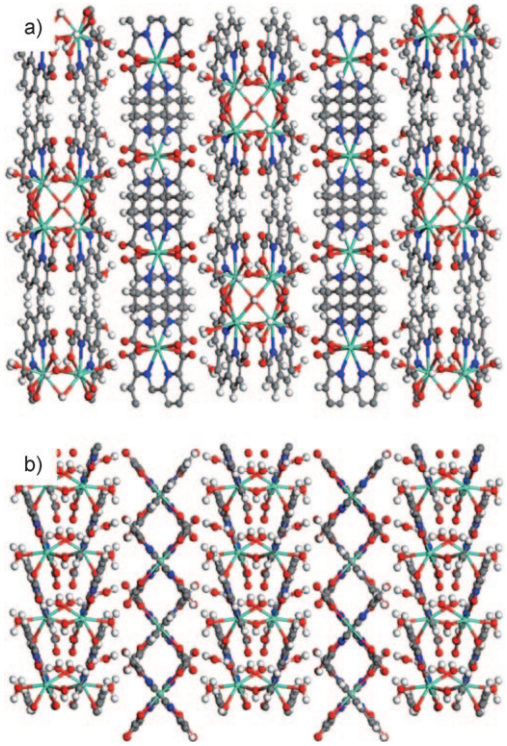

Figure 2. Structure of ITQMOF-3 showing the lamellar packing. a) viewed along the *c* axis. b) viewed along the *a* axis. C gray, H white-gray, N blue, Eu green, O red.

Each Eu^{3+} ion is coordinated by two different ligand molecules to form isolated EuL_2 entities. The L molecule acts as a tetradentate ligand and coordinates the central metal atom through the two N atoms and two O atoms of each carboxylic group. The two ligand molecules connected to the same Eu^{3+} ion lie on 80° planes. Each Eu^{3+} ion is octacoordinated and isolated from the other Eu^{3+} ions in the structure (d_{min} Eu–Eu = 9.51 Å). The ML_2 group interacts with the neighboring groups in the sheet through multiple π–π interactions of the aromatic rings (distance 3.5 Å) to create a two-dimensional self-assembled layer[33] (see Figure S2 in the Supporting Information).

Sheet B contains Eu2 with stoichiometry $[M_2L_2(OH)(OH_2)_4]$, and is thus positively charged. In this case, the sheet is formed by isolated planar chains along the *c* axis. The M atoms form pairs of Eu^{3+} ions connected through an OH group (Eu–O–Eu; d_{Eu-Eu} = 4.61 Å), which also stack along the *c* axis. Each Eu atom is also coordinated by one L molecule that acts as a tetradentate ligand through the two N and two O atoms, one L molecule that coordinates through one O atom while also tetracoordinating an Eu^{3+} ion of a neighboring Eu–O–Eu pair, one OH group that links the Eu^{3+} ions in a couple, and two water molecules. As a result, the Eu2 is also octacoordinated, although in a very different environment from that of Eu1, and are situated close to the neighboring Eu^{3+} ions. The distance between Eu^{3+} ions of different pairs connected through a carboxylic Eu–O–C–O–Eu bridge is 6.49 Å. The linkage between adjacent A and B sheets take place mainly through electrostatic interactions because of their respective negative and positive charges. Last, an additional water molecule that originates from the solvent has been found close to the B sheets.

The ITQMOF-3 material has good thermal stability up to 573 K in air (see Figure S1 in the Supporting Information). In the range 423–500 K, the TGA curve exhibits an initial weight loss of 6.6%, which corresponds approximately to four coordinated water molecules and two free water molecules in the interstitial zone. The material starts to decompose at around 573 K (weight loss 61.5%), as confirmed by variable-temperature powder X-ray diffraction. The transformation continues up to 873 K, where the corresponding lanthanide oxide is the final product.

The excitation spectra of ITQMOF-3-Eu recorded at both room temperature and 12 K (Figure 3a) display a series of

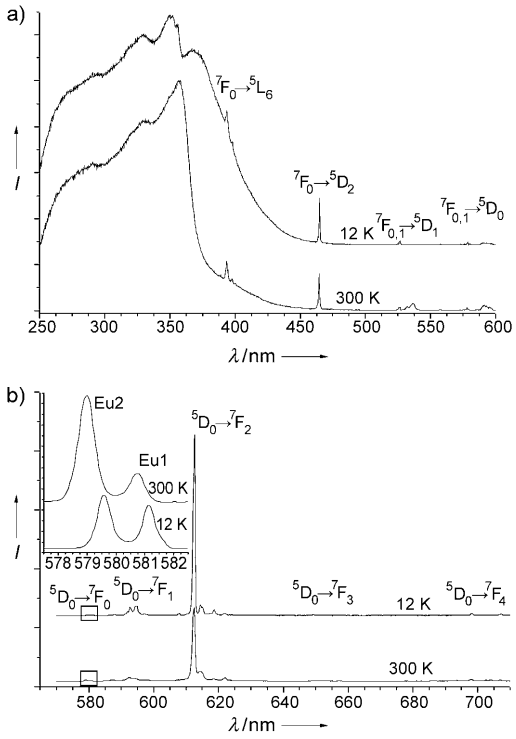

Figure 3. a) Excitation spectra of ITQMOF-3-Eu crystals recorded at 300 K and 12 K with the emission monitored at 612.3 nm. b) Emission spectra of ITQMOF-3-Eu recorded at 300 K and 12 K under 350 nm excitation. The inset shows an expansion of the Eu^{3+} $^5D_0 \rightarrow {}^7F_0$ emission region.

sharp lines assigned to the $^7F_0 \rightarrow {}^5D_{2-0}$ and $^5L_6$ Eu^{3+} intra-$4f^6$ transitions. Moreover, the spectra exhibit several intense and broad bands in the UV region, with a maximum at around 350 nm, which is attributed to ligand excited states.

The sharp lines in the emission spectra (Figure 3b) are assigned to transitions between the first excited non-degenerate $^5D_0$ state and the $^7F_{0-4}$ levels of the fundamental Eu^{3+} septet. The presence of two different Eu^{3+} environments,

which is in agreement with the crystal structure results, is indicated by two lines at approximately 579.0 nm (17272 cm^{-1}) and 580.7 nm (17221 cm^{-1}) in the 300 K spectrum (which are attributed to sites Eu2 and Eu1, respectively) for the nondegenerate $^5D_0 \rightarrow {}^7F_0$ transition (inset in Figure 3b), and the local-field splitting of the $^7F_1$ level into six Stark components (Figure 3b). The photoluminescence features of each site may be rationalized in terms of the relationship between the covalency of the Eu–(O,N) bonds and the nephelauxetic effect that influences the energy of the $^5D_0 \rightarrow {}^7F_0$ transition:[34] a site with more covalent Eu–(O,N) bonds has a $^5D_0 \rightarrow {}^7F_0$ transition at lower energy and a longer emission lifetime. Surprisingly, in contrast with the behavior of site Eu1, the $^5D_0 \rightarrow {}^7F_0$ transition intensity of site Eu2 increases with temperature, (Figure 3b, inset). This behavior is unexpected because a temperature increase promotes the nonradiative processes that quench the emission. The dominant mechanism of the $^5D_0 \rightarrow {}^7F_0$ line (forbidden by electric-dipole and magnetic-dipole rules) is generally attributed to the borrowing of intensity from the hypersensitive $^5D_0 \rightarrow {}^7F_2$ transition through crystal-field-induced J mixing.[35,36] It is well known that the intensity of the hypersensitive $^5D_0 \rightarrow {}^7F_2$ transition varies considerably with the chemical environment.[35] Hence, the increase of the $^5D_0 \rightarrow {}^7F_0$ transition intensity of Eu2 with temperature is likely to arise from changes induced in the local site geometry of the dimers, which is clearly evidenced by the blue shift of the $^5D_0 \rightarrow {}^7F_0$ energy with temperature in the range 12–300 K (Figure 3b, inset). To better understand the different behavior of the two Eu^{3+} sites, we recorded the $^5D_0$ decay curves detected on the two different $^5D_0 \rightarrow {}^7F_0$ transitions at temperatures in the range 12–300 K. At all temperatures, the decay curves obtained by monitoring the Eu1 emission (ca. 580.7 nm) are monoexponential with $^5D_0$ lifetimes in the range (1.03 ± 0.01) ms (12 K) and (0.53 ± 0.01) ms (300 K; see Figure S3 in the Supporting Information). The curves obtained by monitoring the Eu2 emission (ca. 579.0 nm) exhibit a different behavior: 1) at 12 K, the decay curve is monoexponential (with a lifetime of (0.28 ± 0.01) ms); 2) in the range 50–100 K, the curves are biexponential, with one of the lifetimes equal to the lifetime measured by monitoring the Eu1 emission; 3) in the range 150–300 K, the curves are monoexponential and show the lifetime of the Eu1 emission (the $^5D_0$ lifetime of the Eu2 emission is below the detection limit of our equipment, 0.03 ms). These observations indicate the occurrence of thermally activated energy migration from Eu1 to Eu2, with a rate larger than the lifetime of the Eu2 emission. Clearly, the shorter lifetime of the Eu2 emission is ascribed to the presence of two water molecules and a hydroxy group, which strongly quench the radiative emission, in the first coordination sphere of this site.

The absolute emission quantum yield (η) of ITQMOF-3-Eu is very high, with a maximum value of 0.56 at an excitation wavelength of 350 nm. This excellent value supports the good balance between absorption, energy transfer, and emission rates mentioned above, and affords the material real potential for use in sensor miniaturization.

Our preliminary results on the use of ITQMOF-3-Eu as a pH sensor are very encouraging. The sensor has a linear response in the pH range 5–7.5, which is required for work with biological fluids such as blood and culture cell media. At a pH value lower than 4, the protonation of the carboxylic groups takes place followed by irreversible changes in the MOF structure. In contrast, for pH values above 8, europium hydroxide is formed as a result of the competition for the metal coordination sites between the hydroxide groups and the carboxylic groups of the ligand. However, the ITQMOF-3-Eu structure is stable at pH 5–7.5 and the observed changes in the photoluminescence are fully reversible. Most interestingly, this sensor requires no calibration because only one of the two Eu^{3+} emitting sites is affected by the pH variation in the range 5 to 7.5. By following the intensity ratio (I_r) of the $^5D_0$-$^7F_0$ emissions of the two Eu^{3+} types (Eu1 580.7 nm; Eu2 579.0 nm, Figure 4a), it is possible to determine the pH of the solution to be analyzed. In this pH range, the relation between the Eu2/Eu1 (579.0 nm/580.5 nm) peak intensities I_r and the pH value present a good linearity ($R = 0.9997$). By taking advantage of the two main properties of ITQMOF-3-Eu (i.e., high emission quantum efficiency and pH-sensing capability) it was possible to design a new miniaturized pH sensor prototype by combining the material with a commercial fiber optic 1.5 mm in diameter. By using this device, we were able to continuously measure the pH in the range 5–7.5 with a

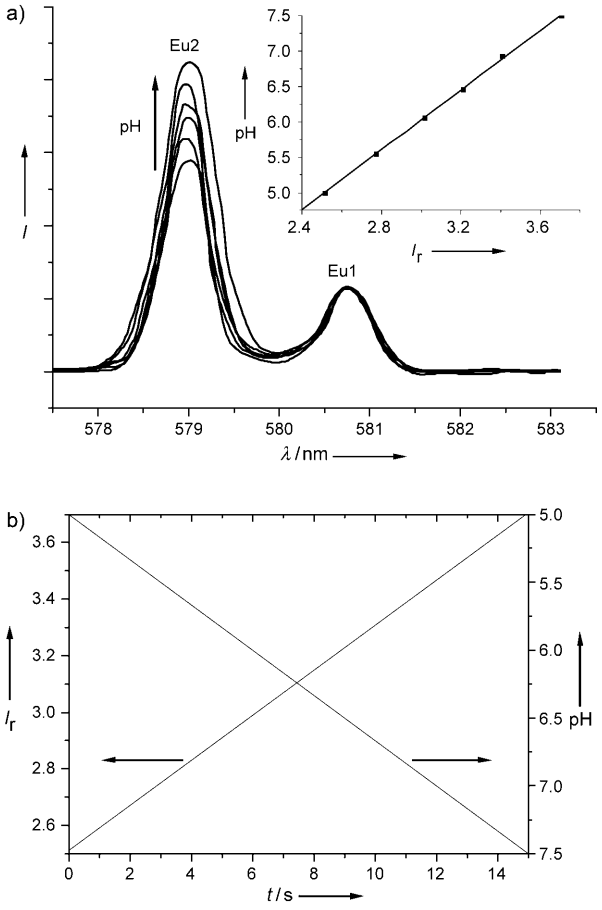

Figure 4. a) Intensity variation of the Eu2 $^5D_0 \rightarrow {}^7F_0$ transition from high (pH 7.5) to low (pH 5) pH values; the inset shows the linear variation of I_r with the pH value. b) Time variation of I_r with the pH change from 5 to 7.5 in ramping mode (measured with a glass electrode).

rapid response between the photoluminescence and the pH variation (Figure 4b).

In conclusion, the careful choice of the ligand and synthesis parameters has enabled the synthesis of a new LnMOF. This material exhibits a high emission quantum yield that made the fabrication of a miniaturized pH sensor viable. The sensor does not require external calibration for the pH range 5–7.5, which is the common range for the study of biological fluids. The same ITQMOF-3 type structure was obtained when other lanthanide ions or mixtures of lanthanide ions were used. The results presented here open new possibilities for the use of these materials as bimodal imaging nanoprobes (MRI contrast agents and luminescent indicators) in biomedical applications.

Received: April 16, 2009
Published online: July 23, 2009

Keywords: carboxylate ligands · lanthanides · luminescence · metal–organic frameworks · sensors

[1] F. Gándara, A. de Andrés, B. Gómez-Lor, E. Gutiérrez-Puebla, M. Iglesias, M. A. Monge, D. M. Proserpio, N. Snejko, *Cryst. Growth Des.* **2008**, *8*, 378–380.
[2] C.-G. Wang, Y.-H. Xing, Z.-P. Li, J. Li, X.-Q. Zeng, M.-F. Ge, S.-Y. Niu, *Cryst. Growth Des.* **2009**, *9*, 1525–1530.
[3] T. Devic, C. Serre, N. Audebrand, J. Marrot, G. Férey, *J. Am. Chem. Soc.* **2005**, *127*, 12788–12789.
[4] Q. Shi, S. Zhang, Q. Wang, H. Ma, G. Yang, W.-H. Sun, *J. Mol. Struct.* **2007**, *837*, 185–189.
[5] F. Gándara, A. Garcia-Cortés, C. Cascales, B. Gómez-Lor, E. Gutiérrez-Puebla, M. Iglesias, M. A. Monge, N. Snejko, *Inorg. Chem.* **2007**, *46*, 3475–3484.
[6] J. Hafizovic, A. Krivokapic, K. C. Szeto, S. Jakobsen, K. P. Lillerud, U. Olsbye, M. Tilset, *Cryst. Growth Des.* **2007**, *7*, 2302–2304.
[7] X. Guo, G. Zhu, Z. Li, F. Sun, Z. Yang, S. Qiu, *Chem. Commun.* **2006**, 3172–3174.
[8] Z. Zheng, *Chem. Commun.* **2001**, 2521–2529.
[9] N. Snejko, C. Cascales, B. Gómez-Lor, E. Gutiérrez-Puebla, M. Iglesias, C. Ruiz-Valero, M. A. Monge, *Chem. Commun.* **2002**, 1366–1367.
[10] J. Perles, M. Iglesias, C. Ruiz-Valero, N. Snejko, *J. Mater. Chem.* **2004**, *14*, 2683–2689.
[11] F. X. Llabrés i Xamena, A. Abad, A. Corma, H. Garcia, *J. Catal.* **2007**, *250*, 294–298.
[12] F. X. Llabrés i Xamena, O. Casanova, R. Galiasso Tailleur, H. Garcia, A. Corma, *J. Catal.* **2008**, *255*, 20–227.
[13] F. X. Llabrés i Xamena, A. Corma, H. Garcia, *J. Phys. Chem. C* **2007**, *111*, 80–85.
[14] B. Chen, Y. Yang, F. Zapata, G. Lin, G. Qian, E. B. Lobkovsky, *Adv. Mater.* **2007**, *19*, 1693–1696.
[15] L.-Z. Zhang, W. Gu, B. Li, X. Liu, D.-Z. Liao, *Inorg. Chem.* **2007**, *46*, 622–624.
[16] W.-H. Zhu, Z.-M. Wang, S. Gao, *Inorg. Chem.* **2007**, *46*, 1337–1342.
[17] B. Chen, L. Wang, F. Zapata, G. Qian, E. B. Lobkovsky, *J. Am. Chem. Soc.* **2008**, *130*, 6718–6719.
[18] B. Chen, L. Wang, Y. Xiao, F. R. Fronczek, M. Xue, Y. Cui, G. Qian, *Angew. Chem.* **2009**, *121*, 508–511; *Angew. Chem. Int. Ed.* **2009**, *48*, 500–503.
[19] B. V. Harbuzaru, A. Corma, F. Rey, P. Atienzar, J. L. Jordá, H. García, D. Ananias, L. D. Carlos, J. Rocha, *Angew. Chem.* **2008**, *120*, 1096–1099; *Angew. Chem. Int. Ed.* **2008**, *47*, 1080–1083.
[20] W. J. Rieter, K. M. L. Taylor, H. An, W. Lin, W. Lin, *J. Am. Chem. Soc.* **2006**, *128*, 9024–9025.
[21] J. Zhang, Z.-J. Li, X.-Y. Cao, Y.-G. Yao, *J. Mol. Struct.* **2005**, *750*, 39–43.
[22] J.-m. Shi, W. Xu, Q.-y. Liu, F.-l. Liu, Z.-l. Huang, H. Lei, W.-t. Yuc, Q. Fang, *Chem. Commun.* **2002**, 756–757.
[23] T. Jüstel, H. Nikol, C. Ronda, *Angew. Chem.* **1998**, *110*, 3250–3271; *Angew. Chem. Int. Ed.* **1998**, *37*, 3084–3103.
[24] C. Seward, N.-X. Hu, S. Wang, *J. Chem. Soc. Dalton Trans.* **2001**, 134–137.
[25] M. Alvaro, V. Fornes, S. Garcia, H. Garcia, J. C. Scaiano, *J. Phys. Chem. B* **1998**, *102*, 8744–8750.
[26] J. Coates, P. G. Sammes, R. M. West, *J. Chem. Soc. Perkin Trans. 2* **1996**, 1275–1282.
[27] J. Coates, P. G. Sammes, R. M. West, *J. Chem. Soc. Perkin Trans. 2* **1996**, 1283–1287.
[28] P. J. Hagrman, D. Hagrman, J. Zubieta, *Angew. Chem.* **1999**, *111*, 2798–2848; *Angew. Chem. Int. Ed.* **1999**, *38*, 2638–2684.
[29] S. Thushari, J. A. K. Cha, H.-Y. Sung, S. S.-Y. Chui, A. L.-F. Leung, Y.-F. Yen, I. D. Williams, *Chem. Commun.* **2005**, 5515–5517.
[30] Crystal data for ITQMOF-3-Eu $[Eu_3(C_{14}H_6N_2O_4)_4(OH)(H_2O)_4]\cdot 2H_2O$; $M_r = 1645.83$; orthorhombic, space group $Ccc2$ (37); $a = 15.625(5)$, $b = 31.237(5)$, $c = 10.847(5)$ Å, $V = 5294(3)$ Å^3; $Z = 4$, $\rho = 2.065$ g cm^{-3}. CCDC 737081 contains the supplementary crystallographic data for this paper. These data can be obtained free of charge from The Cambridge Crystallographic Data Centre via www.ccdc.cam.ac.uk/data_request/cif.
[31] G. M. Sheldrick, SHELXS-97 (Release 97–2), A Program for Automatic Solution of Crystal Structures. University of Göttingen, Germany, **1997**.
[32] G. M. Sheldrick, SHELXL-97 (Release 97–2), A Program for Crystal Structure Refinement, University of Göttingen, Germany, **1997**.
[33] A. Corma, F. Rey, J. Rius, M. J. Sabater, S. Valencia, *Nature* **2004**, *431*, 287–290.
[34] L. D. Carlos, R. A. S. Ferreira, V. de Zea Bermudez, S. J. L. Ribeiro, *Adv. Mater.* **2009**, *21*, 509–534.
[35] O. L. Malta, W. M. Azevedo, E. A. Gouveia, G. F. de Sá, *J. Lumin.* **1982**, *26*, 337–343.
[36] T. Masanori, N. Goro, K. Takashi, *Phys. Rev. B* **1994**, *49*, 16917–16925.

